Poly(L-Lactic Acid)/Silicon Dioxide Nanocomposite Prepared Via the *In Situ* Melt Polycondensation of L-Lactic Acid in the Presence of Acidic Silica Sol: Isothermal Crystallization and Melting Behaviors

Dan Cao, Linbo Wu

State Key Laboratory of Polymer Reaction Engineering, Institute of Polymer Engineering, College of Materials and Chemical Engineering, Zhejiang University, Hangzhou 310027, China

Received 15 January 2008; accepted 30 July 2008
DOI 10.1002/app.29017
Published online 17 October 2008 in Wiley InterScience (www.interscience.wiley.com).

ABSTRACT: In a previous article, we reported the preparation and characterization of a nanocomposite of poly(L-lactic acid) (PLLA) and silica via the *in situ* melt polymerization of L-lactic acid in the presence of acidic silica sol. In this study, the isothermal crystallization and melting behaviors of a PLLA/silicon dioxide (SiO_2) nanocomposite with 5 wt % well-dispersed SiO_2 nanoparticles (PLLASN5) and pure PLLA were comparatively studied with differential scanning calorimetry and polarized optical microscopy. The SiO_2 nanoparticles acted as nucleation agents in the PLLA matrix and enhanced its nucleation rate and overall crystallization rate, especially at high crystallization temperatures. However, no deleterious effect on the crystal morphology or crystallinity was observed. The crystals that formed at a low temperature were imperfect; therefore, double melting peaks occurred during the second heating scan because of melt recrystallization. With the crystallization temperature increasing, the crystals became increasingly perfect; as a result, the low melting peak increased and shifted to a higher temperature. The existence of SiO_2 nanoparticles had no effect on the equilibrium temperature of the PLLA matrix. Pure PLLA and PLLASN5 have the same equilibrium temperature of 171.5°C. © 2008 Wiley Periodicals, Inc. J Appl Polym Sci 111: 1045–1050, 2009

Key words: biodegradable; crystallization; melt; nanocomposites; polyesters

INTRODUCTION

Poly(L-lactic acid) (PLLA) is a biodegradable and biocompatible aliphatic polyester produced from renewable resources such as corn starch. Generally, PLLA possesses good physical and mechanical properties and can be used in packing materials, fibers, agricultural films, and biomaterials.[1–4] However, its thermal stability, toughness, and gas-barrier properties still need to be improved for more widespread applications. For property improvement, PLLA nanocomposites with layered silicates (LSs) have been extensively researched in recent years.[5–18] The modulus and flexible properties, heat distortion temperature, oxygen gas permeability, and degradation rate have been improved considerably.[5,9,15] PLLA nanocomposites with hydroxyapatite,[19,20] carbon nanotubes,[21,22] and silicon dioxide (SiO_2)[23–25] have also been reported.

In addition to the interfacial interaction between the PLLA matrix and the nanofillers, the crystalline properties and melting behaviors of the PLLA matrix and the effect of nanofillers on them are crucial for the properties and end use of PLLA nanocomposites. For PLLA and its nanocomposites prepared via melt polycondensation,[25,26] a subsequent solid-state polycondensation is often needed to increase the molecular weight.[27,28] During this process, the crystalline properties of the PLLA matrix have a significant effect on its molecular weight growth.[28] Therefore, a thorough understanding of the crystallization and melting behaviors of PLLA nanocomposites is of great significance. Nam et al.[13] reported the crystallization behavior and morphology of a PLLA/LS nanocomposite and found that the intercalated LS particles acted as a nucleating agent. Their existence resulted in a more rapid overall crystallization rate, an unchanged linear growth rate, and poor ordering of spherulites. In a PLLA/multiwalled carbon nanotube nanocomposite, it was found that the multiwalled carbon nanotubes also enhanced the crystallization of the PLLA matrix.[21,29]

Correspondence to: L. Wu (wulinbo@zju.edu.cn).

Contract grant sponsor: National Science Foundation of China; contract grant numbers: 20406018, 20304012, and 20674067.

Contract grant sponsor: Prior Special Fund of the National Basic Research Program of China; contract grant number: 2004CCA05500.

Contract grant sponsor: Natural Science Foundation of Zhejiang Province; contract grant number: Y404084.

Until now, most PLLA nanocomposites have been prepared via melt blending,[5–14,16,17] *in situ* ring-opening polymerization of L-lactide,[18] or a sol–gel method.[24] The research on the crystallization and melting behaviors is also mainly based on such products.[13,29] In a previous article,[25] we reported the preparation and characterization of a PLLA/SiO_2 nanocomposite via the *in situ* melt polycondensation of L-lactic acid in the presence of acidic silica sol (aSS). In this study, we report its isothermal crystallization and melting behaviors in comparison with those of pure PLLA.

EXPERIMENTAL

Materials

Pure PLLA and a PLLA/SiO_2 nanocomposite with 5 wt % SiO_2 nanoparticles (PLLASN5) were comparatively studied in this work. The samples were prepared via the *in situ* melt polycondensation of L-lactic acid (LLA) with or without aSS, as reported previously.[25] The weight-average molecular weights of the pure PLLA and the PLLA matrix in PLLASN5 were 102,000 and 109,900 (based on polystyrene standards), respectively. Their polydispersity was nearly 1.5.

Transmission electron microscopy (TEM)

TEM (JEM-1230, JOEL, Japan) was used to observe the dispersion of SiO_2 nanoparticles in PLLASN5. The specimens were prepared by ultrathin sectioning. The ultrathin section (ca. 80 nm) was supported by a TEM copper grid for TEM observation.

Polarized optical microscopy (POM)

The spherulite morphology and growth rate of PLLA and PLLASN5 were studied with a Nikon (Japan) E600 POL polarized optical microscope equipped with a Linkam THMS600 hot stage (Linkham Scientific Instrument Ltd., England) and a digital camera system. The sample ($\sim$ 0.5 mg) was made into a film with a thickness less than 10 μm on the hot stage by being melted on a slide glass and pressed with a cover glass. The film was heated to 200°C, maintained at 200°C for 3 min, and then cooled at 80°C/min to a programmed temperature to observe the growth and morphology of the spherulites.

Thermal analysis

The isothermal cold crystallization and melting behaviors of PLLA and PLLASN5 were studied with a PerkinElmer DSC7 system (Waltham, MA) under an N_2 atmosphere. The differential scanning calorimetry (DSC) instrument was calibrated with the melting temperature and enthalpy of indium, the standard material. The sample was first heated from 30 to 200°C at 10°C/min and maintained at 200°C for 3 min, then cooled to 30°C at −80°C/min and maintained at 30°C for 3 min, and finally heated at 80°C/min from 30°C to the isothermal crystallization temperature (T_c to 110–140°C) to perform isothermal crystallization for 8–15 min. After the crystallization was completed, the sample was reheated to 200°C at 10°C/min to observe the melting behavior. For the calculation of the crystallinity of PLLASN5, the crystallization enthalpy given by DSC [$\Delta H_{c,\ DSC}$ (J/g of nanocomposite)] was divided by 0.95 to be converted to the true value [$\Delta H_c = \Delta H_{c,\ DSC}/0.95$ (J/g of PLLA)], given that there was 5 wt % SiO_2 in the nanocomposite.

RESULTS AND DISCUSSION

Nanocomposite structure

A representative PLLA/SiO_2 nanocomposite with 5 wt % SiO_2 nanoparticles (PLLASN5) was used for a comparative study of the crystallization and melting behaviors of pure PLLA. It was prepared via the *in situ* melt polycondensation of L-lactic acid in the presence of aSS, as reported previously.[25] Because of the ease of dispersion of aSS in the aqueous L-lactic acid monomer and *in situ* grafting of oligo(L-lactic acid) onto the surface of the SiO_2 nanoparticles, the nanoparticles could be well dispersed on a nanoscale in the PLLA matrix.[25] Figure 1 shows a TEM micrograph of PLLASN5. It clearly demonstrates a nanoscale dispersion of SiO_2 in the nanocomposite. As a result, the transmittance of the amorphous film of PLLASN5 was comparable to that of the pure PLLA

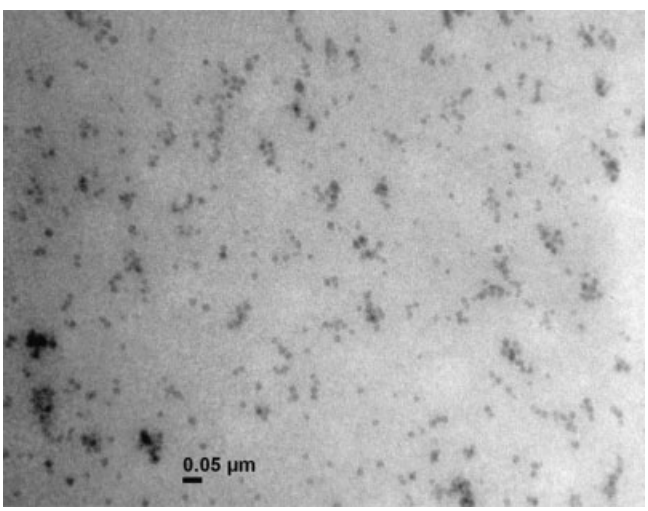

Figure 1 Typical TEM micrograph of PLLASN5.

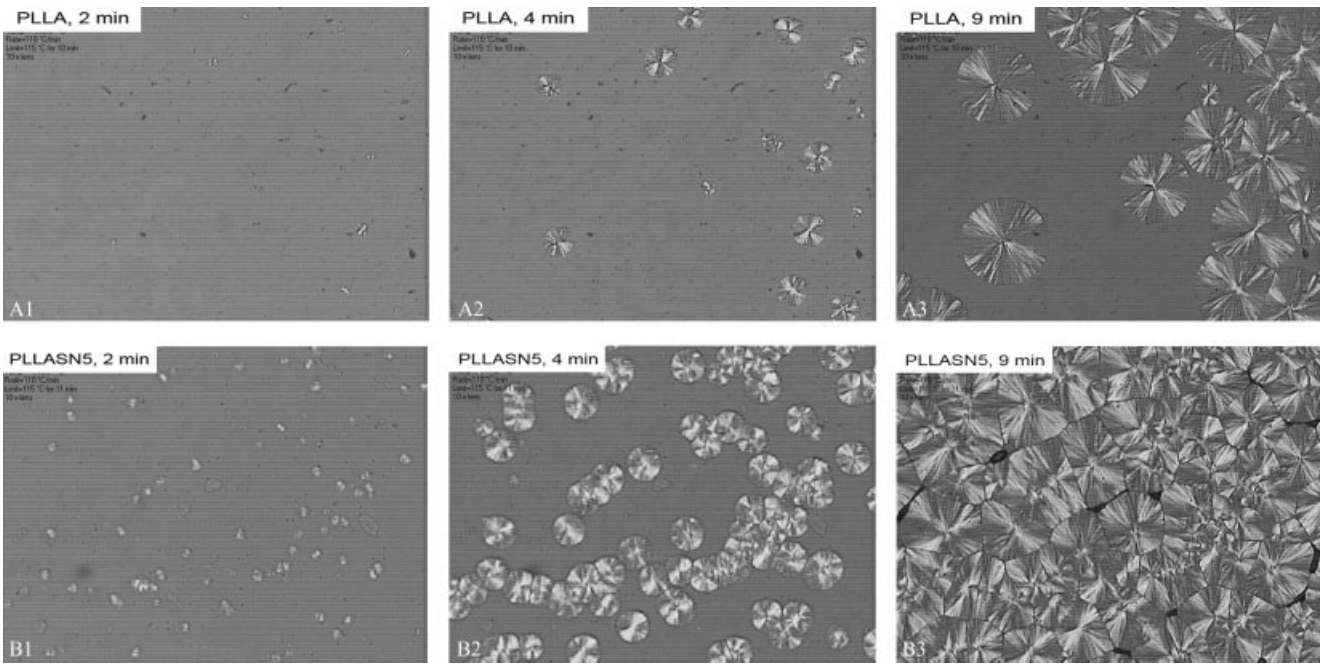

Figure 2 POM micrographs of spherulites in PLLA and PLLASN5 after crystallization at 115°C for 2, 4, and 9 min.

film in the visible light range (390–770 nm).[25] In addition, the molecular weights of pure PLLA and the PLLA matrix in PLLASN5 were approximately identical.

Spherulite morphology and growth rate

Nanoparticles in polymer nanocomposites usually act as nucleating agents for crystallization.[13,30] To get direct evidence of the nucleation effect of SiO_2 nanoparticles in the PLLA/SiO_2 nanocomposite, the formation and growth of crystals were observed with POM. Figure 2 shows micrographs of pure PLLA and PLLASN5 formed after isothermal melt crystallization at 115°C for 2, 4, and 9 min. Spherulite crystals were formed in both pure PLLA and PLLASN5. The spherulites appeared earlier and their number was clearly greater in PLLASN5 than in pure PLLA. This indicated that the well-dispersed SiO_2 nanoparticles acted as nucleation agents and promoted the nucleation in PLLASN5. The effect of a nanofiller on the spherulite morphology may depend on its shape. The existence of zero-dimensional spherical SiO_2 nanoparticles did not have a deleterious effect on the spherulite morphology of PLLA. Even a little more perfect morphology can be observed in Figure 2. However, it has been reported that less ordered spherulites are formed in nanocomposites of PLLA and two-dimensional LSs.[13]

The spherulite radii of both PLLA and PLLASN5 grew linearly with time at various T_c's, as shown in Figure 3. It is interesting that the growth rate of PLLASN5 appeared to be higher than that of PLLA, reaching 1.5 times its value except at 110°C. Figure 2 also shows that larger spherulites were formed in the same crystallization time. This result differs from the report that LS has no effect on the growth rate of a PLLA matrix in a PLLA/LS nanocomposite, although it also acts as a nucleation agent.[13] The reason is not clear yet. However, it may be a desirable result because in addition to the nucleation effect, it provides an additional means of enhancing the slow rate of the melt crystallization of PLLA.

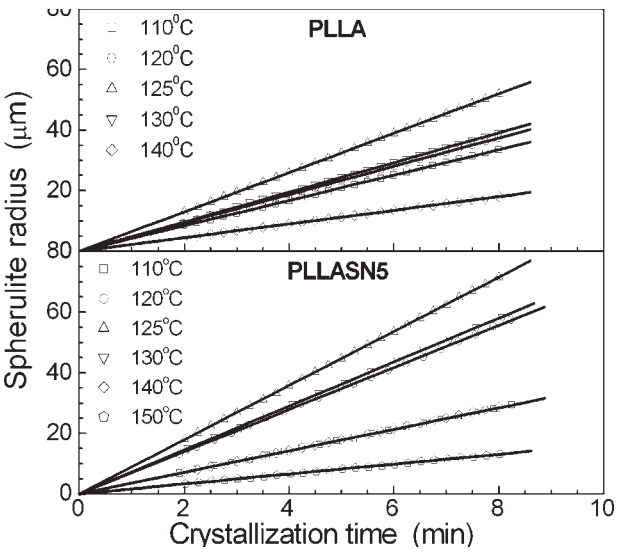

Figure 3 Growth of the spherulite radius of pure PLLA and PLLASN5 with time at various T_c's.

Isothermal cold crystallization

The weight-average molecular weight of the PLLA/SiO_2 nanocomposite prepared by our method reached about 100,000 and could be further increased by a subsequent solid-state polycondensation. To reach the crystallinity necessary to facilitate solid-state polycondensation, a cold crystallization pretreatment is usually necessary.[27,28] Therefore, we studied the isothermal cold crystallization and subsequent melting behaviors with emphasis.

Figure 4 shows the DSC curves of the isothermal cold crystallization of PLLA and PLLASN5 at temperatures ranging from 110 to 140°C. Although our observations (data not shown) and another's report[31] have shown that the melt crystallization of PLLA is quite slow, its cold crystallization was quite rapid. It was finished within 3–10 min. PLLASN5 crystallized more rapidly, and the crystallization time was only 1.5–3 min. The overall crystallization rate [reciprocal of the half-crystallization time ($t_{1/2}^{-1}$)] of PLLASN5 was obviously higher than that of PLLA, as shown in Figure 5. The maximum crystallization temperature ($T_{c,\max}$) shifted from 120°C for PLLA to 125°C for PLLASN5. The corresponding half-crystallization times at $T_{c,\ \max}$ were 1.3 and 0.5 min, respectively.

To illustrate the effect of temperature on the increase in the crystallization rate, the $t_{1/2}^{-1}$ ratio for PLLASN5 and PLLA is also plotted in Figure 5. The result indicates that the increase in the crystallization rate became more significant at higher T_c's. $t_{1/2}^{-1}$ of PLLASN5 was more than twice that of PLLA at 110°C and over 3 times greater at 140°C. As for pure PLLA, its nucleation rate was considerable at relatively low temperatures, but the crystal nuclei were more difficult to form and stabilize at higher temperatures because of the thermal movement of the polymer chains. As a result, the nucleation rate and the overall crystallization rate increased to a greater extent at a higher temperature after the introduction of SiO_2 nanoparticles because of its more significant nucleation effect.

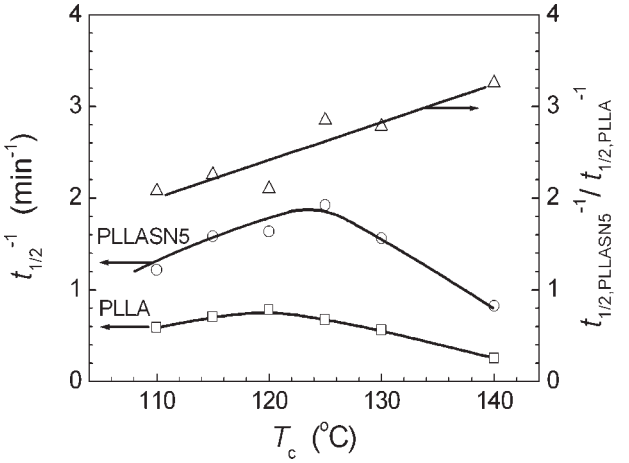

Figure 5 Overall crystallization rates of PLLASN5 ($t_{1/2,\mathrm{PLLASN5}}^{-1}$) and PLLA ($t_{1/2,\mathrm{PLLA}}^{-1}$) and their ratios ($t_{1/2,\mathrm{PLLASN5}}^{-1}/t_{1/2,\mathrm{PLLA}}^{-1}$) at various temperatures.

Although PLLASN5 crystallized more rapidly than PLLA, its crystallization enthalpy was nearly the same as that of PLLA, as illustrated in Figure 6. T_c did not exhibit a clear effect on the crystallization enthalpy. The average was 47.2 ± 2.6 J/g. According to the melting enthalpy of PLLA with 100% crystallinity (93 J/g),[32] the crystallinity of PLLA and PLLSN5 after isothermal cold crystallization reached 50.7 ± 2.9%.

Crystallization kinetics are usually described with the Avrami equation:

$$\log[-\ln(1 - x_t)] = \log K + n \log t \qquad (1)$$

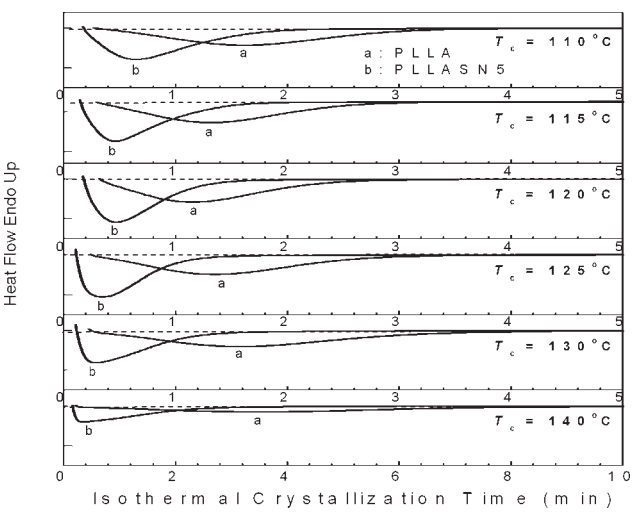

Figure 4 DSC curves for the isothermal cold crystallization of PLLA and PLLASN5 at various temperatures.

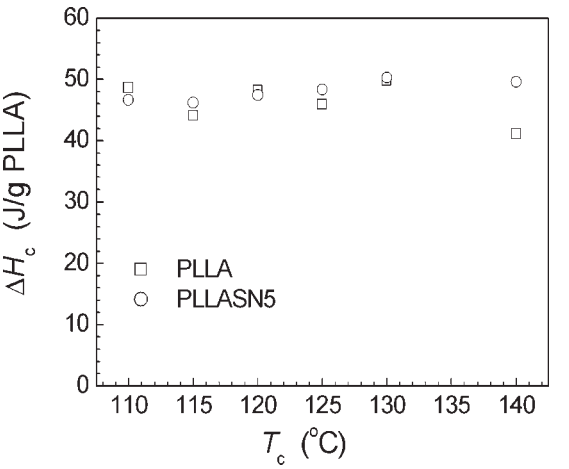

Figure 6 ΔH_c of PLLASN5 and PLLA at various temperatures.

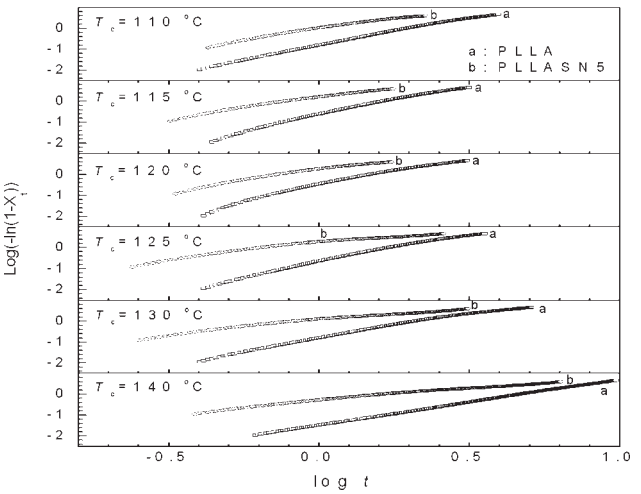

Figure 7 Avrami plots of the isothermal cold crystallization of PLLA and PLLASN5 at various temperatures.

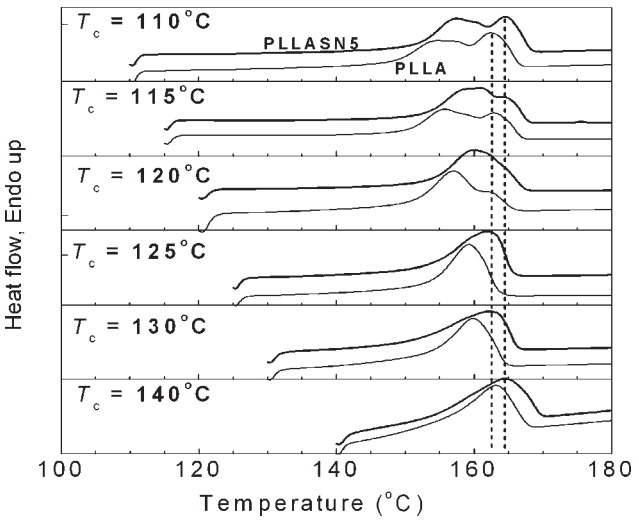

Figure 8 DSC curves of the second heating scan (10°C/min) of PLLA and PLLASN5 after isothermal crystallization at various temperatures.

where x_t is the relative crystallinity at time t, K is the crystallization rate constant, and n is the Avrami exponent. x_t is calculated as follows:

$$x_t = \frac{\int_0^t \left(\frac{dH_c}{dt}\right)dt}{\int_0^\infty \left(\frac{dH_c}{dt}\right)dt} \quad (2)$$

where dH_c/dt is the heat flow. Figure 7 shows the Avrami plots of PLLA and PLLASN5. It can be seen that the crystallization of PLLA basically agreed with the Avrami equation, except at the end of the crystallization process. The Avrami exponents of PLLA were close to 3, except at 140°C (ca. 2.2). However, PLLASN5 departed from the linear relationship earlier and more clearly. The Avrami exponents were roughly estimated to be close to 2 at $T_c < 120$°C and less than 2 at $T_c > 120$°C. Obviously, the crystallization rate constant of PLLASN5 was higher than that of PLLA.

Melt behavior

The DSC curves after isothermal crystallization are shown in Figure 8. Double melting peaks were observed for both PLLA and PLLASN5 after crystallization at a low T_c. Single melting peaks occurred at T_c's over 120°C. The area of the low melting peak increased but that of the high melting peak decreased with increasing T_c. When the high melting peaks disappeared, the single melting peaks appeared. In other words, the single melting peaks can be regarded as the evolution of the low melting peaks at a high T_c. The peak temperature of the high melting peaks (T_{mH}) remained almost unchanged (162.6 ± 0.5°C for PLLA and 164.4 ± 0.2°C for PLLASN5 at T_c = 110–120°C). However, the peak temperature of the low and single melting peaks (T_{mL}) increased continuously with increasing T_c and reached T_{mH} at $T_c = 140$°C.

The occurrence of double melting peaks in DSC measurements has been reported for PLLA[33] and many other polymers[34,35] as well as PLLA nanocomposites.[29] The phenomenon has been interpreted with a melt–recrystallization model[33,34] and a double-lamellar-thickness model.[29] From the changes of the area and peak temperature of the double peaks, the melt–recrystallization model appears to be reasonable and applicable to PLLA and PLLA/SiO_2 nanocomposites. The crystals that formed at a low T_c were not perfect, so they were melted at T_{mL}, recrystallized to improve the perfection, and as a result, remelted at T_{mH}. As T_c increased, the crystals that formed became increasingly perfect; therefore,

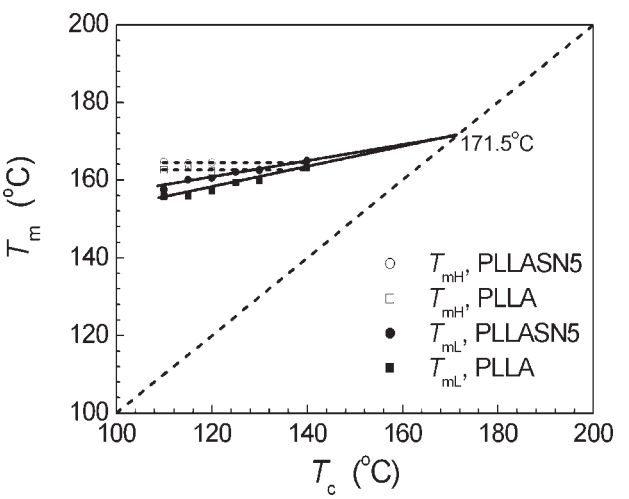

Figure 9 T_m of the crystals formed after the isothermal crystallization of PLLA and PLLASN5 as a function of T_c.

the area of the low melting peak increased but that of the high melting peak decreased until a single peak appeared. T_{mL} and the peak temperature of the single peaks (both denoted T_{mL} in Fig. 9) represent the melting of the crystals directly formed in the isothermal crystallization process. They increased nearly linearly with T_c (Hoffman–Weeks plot), as shown in Figure 9, indicating the increasing perfection of the crystals that formed. It can also be seen that the melting temperature (single peaks) of the crystals that formed at 140°C was equal to T_{mH} of the crystals that formed at 110–120°C. This result suggests that the crystals that formed at $T_c = 140$°C were as perfect as those generated after recrystallization of the crystals that formed at $T_c = 110$–120°C.

The melting temperature of PLLASN5 seemed to be a little higher than that of PLLA, possibly because of a little more perfect crystal morphology. This is in accordance with the observation of Figure 2. However, their equilibrium melting temperatures were the same: 171.5°C.

CONCLUSIONS

The isothermal crystallization and melting behaviors of a PLLA/SiO_2 nanocomposite with 5 wt % well dispersed nanoparticles that was prepared via the *in situ* melt polymerization of L-lactic acid in the presence of aSS were studied. The well-dispersed SiO_2 nanoparticles acted as nucleation agents in the PLLA matrix and enhanced the nucleation rate and overall crystallization rate. The nucleation effect seemed to be more significant at high T_c's. The existence of SiO_2 nanoparticles had no deleterious effect on the crystal morphology or crystallinity of the PLLA matrix in comparison with pure PLLA. During the second heating scan, double melting peaks occurred because of melt recrystallization of the imperfect crystals that formed at low T_c's. With increasing T_c, the crystals became increasingly perfect; as a result, the low melting peak increased and shifted to a higher temperature. The low melting temperatures of PLLA and PLLASN5 both increased linearly with T_c and were extrapolated to the same equilibrium temperature of 171.5°C.

References

1. Drumright, R. E.; Gruber, P. R.; Henton, D. E. Adv Mater 2000, 12, 1841.
2. Sodergard, A.; Stolt, M. Progress Polym Sci 2002, 27, 1123.
3. Bendix, D. Polym Degrad Stab 1998, 59, 129.
4. Kovalchuk, A.; Fischer, W.; Epple, M. Macromol Biosci 2005, 5, 289.
5. Ray, S. S.; Yamada, K.; Okamoto, M.; Ueda, K. Nano Lett 2002, 2, 1093.
6. Ray, S. S.; Maiti, P.; Okamoto, M.; Yamada, K.; Ueda, K. Macromolecules 2002, 35, 3104.
7. Ray, S. S.; Yamada, K.; Okamoto, M.; Ueda, K. Polymer 2003, 44, 857.
8. Ray, S. S.; Yamada, K.; Okamoto, M.; Ogami, A.; Ueda, K. Chem Mater 2003, 15, 1456.
9. Ray, S. S.; Yamada, K.; Ogami, A.; Okamoto, M.; Ueda, K. Macromol Rapid Commun 2002, 23, 943.
10. Maiti, P.; Yamada, K.; Okamoto, M.; Ueda, K.; Okamoto, K. Chem Mater 2002, 14, 4654.
11. Ray, S. S.; Yamada, K.; Okamoto, M.; Fujimoto, Y.; Ogami, A.; Ueda, K. Polymer 2003, 44, 6633.
12. Ray, S. S.; Okamoto, M. Macromol Mater Eng 2003, 288, 936.
13. Nam, J. Y.; Ray, S. S.; Okamoto, M. Macromolecules 2003, 36, 7126.
14. Ray, S. S.; Yamada, K.; Okamoto, M.; Ueda, K. Macromol Mater Eng 2003, 288, 203.
15. Ray, S. S.; Okamota, M. Macromol Rapid Commun 2003, 24, 815.
16. Pluta, M. Polymer 2004, 45, 8239.
17. Pluta, M.; Galeski, A.; Alexandre, M.; Paul, M. A.; Dubios, P. J Appl Polym Sci 2002, 86, 1497.
18. Paul, M. A.; Alexandre, M.; Degee, P.; Calberg, C.; Jerome, R.; Dubois, P. Macromol Rapid Commun 2003, 24, 561.
19. Hong, Z. H.; Zhang, P. B.; Qiu, X. Y.; Qiu, X. Y.; Liu, A. X.; Chen, L.; Chen, X. S.; Jing, X. B. Biomaterials 2005, 26, 6296.
20. Deng, X. M.; Hao, J. Y.; Wang, C. S. Biomaterials 2001, 22, 2867.
21. Moon, S.-I.; Jin, F. Z.; Lee, C.-J.; Tsutsumi, S.; Hyon, S.-H. Macromol Symp 2005, 224, 287.
22. Chen, G. X.; Kim, H.-S.; Park, B. H.; Yoon, J.-S. J Phys Chem B 2005, 109, 22237.
23. Yan, S. F.; Yin, J. B.; Yang, Y.; Dai, Z. Z.; Ma, J.; Chen, X. S. Polymer 2007, 48, 1688.
24. Perry, C. C.; David, E. Mater Res Soc Symp Proc 2002, 726, 67.
25. Wu, L. B.; Cao, D.; Huang, Y.; Li, B.-G. Polymer 2008, 49, 742.
26. Moon, S.-I.; Lee, C. W.; Miyamoto, M.; Kimura, Y. J Polym Sci Part A: Polym Chem 2000, 38, 1673.
27. Moon, S.-I.; Lee, C.-W.; Taniguchia, I.; Miyamotoa, M.; Kimura, Y. Polymer 2001, 42, 5059.
28. Moon, S.-I.; Taniguchi, I.; Miyamoto, M.; Kimura, Y.; Lee, C.-W. High Perform Polym 2001, 13, S189.
29. Shieh, Y.-T.; Liu, G.-L. J Polym Sci Part B: Polym Phys 2007, 45, 1870.
30. Maiti, P.; Nam, P. H.; Okamoto, M.; Kotaka, T.; Hasegawa, N.; Usuki, A. Macromolecules 2002, 35, 2042.
31. Iannace, S.; Nicolais, L. J Appl Polym Sci 1997, 64, 911.
32. Fischer, E. W.; Sterzel, H. J.; Wegner, G. Kolloid Z Z Polym 1973, 251, 980.
33. Yasuniwa, M.; Tsubakihara, S.; Sugimoto, Y.; Nakafuku, C. J Polym Sci Part B: Polym Phys 2004, 42, 25.
34. Holdsworth, P. J.; Turner-Jones, A. Polymer 1971, 12, 195.
35. Sauer, B. B.; Kampert, W. G.; Blanchard, E. N.; Threefoot, S. A.; Hsiao, B. S. Polymer 2000, 41, 1099.